

摩擦学学报

TRIBOLOGY



绳股结构对螺旋接触钢丝间微动摩擦磨损特性影响

徐春明, 彭玉兴, 王燕锋, 张立伟

Influence of Strand Structure on Fretting Friction and Wear Characteristics between Spiral Contact Steel Wires

XU Chunming, PENG Yuxing, WANG Yanfeng, ZHANG Liwei

在线阅读 View online: <https://doi.org/10.16078/j.tribology.2022196>

您可能感兴趣的其他文章

Articles you may be interested in

考虑微动磨损的钢丝微动疲劳裂纹扩展寿命预测研究

Prediction of Fretting Fatigue Crack Propagation Life of Steel Wire Considering Fretting Wear

摩擦学学报. 2021, 41(5): 710 <https://doi.org/10.16078/j.tribology.2021157>

微动频率对钢丝拉扭复合微动腐蚀疲劳行为影响研究

Effect of Fretting Frequency on Tension-Torsion Fretting Corrosion Fatigue Behavior of Steel Wire

摩擦学学报. 2021, 41(6): 964 <https://doi.org/10.16078/j.tribology.2021175>

丝径对316L不锈钢丝摩擦磨损行为的影响

Effect of Wire Diameter on Friction and Wear Behavior of 316L Stainless Steel Wire

摩擦学学报. 2021, 41(2): 206 <https://doi.org/10.16078/j.tribology.2020101>

定、变载弯曲疲劳钢丝绳失效机理对比研究

Comparative Research on Failure Mechanisms of Steel Wire Ropes during Bending Fatigue under Constant and Variable Loads

摩擦学学报. 2020, 40(6): 762 <https://doi.org/10.16078/j.tribology.2020085>

缠绕提升钢丝绳绕入冲击摩擦特性研究

Winding-in Impact Friction Characteristics of Wire Rope in Winding Hoist

摩擦学学报. 2017, 37(1): 90 <https://doi.org/10.16078/j.tribology.2017.01.012>



关注微信公众号, 获得更多资讯信息

DOI: 10.16078/j.tribology.2022196

绳股结构对螺旋接触钢丝间微动摩擦磨损特性影响

徐春明^{1*}, 彭玉兴^{2,3}, 王燕锋¹, 张立伟¹

(1. 宿迁学院 机电工程学院, 江苏 宿迁 223800;

2. 中国矿业大学 机电工程学院, 江苏 徐州 221116;

3. 江苏省矿山智能采掘装备协同创新中心(省部共建), 江苏 徐州 221116)

摘要: 钢丝间微动磨损会加剧提升钢丝绳的疲劳损伤, 降低钢丝绳的使用寿命, 严重威胁矿井提升安全. 为了研究绳股结构对螺旋接触钢丝间微动摩擦磨损特性的影响, 在自制试验台上开展了拉伸-扭转耦合力作用下钢丝微动磨损试验. 结果显示: 随着接触力增加, 相同直径接触对下钢丝间摩擦系数从0.748减小到0.646, 而不同直径接触对下钢丝间摩擦系数从0.941减小到0.911; 相比于凹接触对, 凸接触对下钢丝表面磨损更加严重, 并且不同直径钢丝间磨损深度和磨损系数明显大于相同直径钢丝间磨损深度和磨损系数; 钢丝间主要磨损机理为磨粒磨损、黏着磨损和疲劳磨损, 并且不同直径接触对下钢丝表面疲劳磨损特征更加严重; 钢丝疲劳断口的瞬断区存在大量二次裂纹和韧窝形貌, 钢丝疲劳断裂失效机理主要为韧性断裂.

关键词: 钢丝; 绳股结构; 微动磨损; 磨损机理; 断裂失效

中图分类号: TH117.1

文献标志码: A

文章编号: 1004-0595(2023)10-1175-14

Influence of Strand Structure on Fretting Friction and Wear Characteristics between Spiral Contact Steel Wires

XU Chunming^{1*}, PENG Yuxing^{2,3}, WANG Yanfeng¹, ZHANG Liwei¹

(1. School of Mechatronic Engineering, Suqian University, Jiangsu Suqian 223800, China;

2. School of Mechatronic Engineering, China University of Mining and Technology, Jiangsu Xuzhou 221116, China;

3. Jiangsu Province and Education Ministry Co-sponsored Collaborative Innovation Center of Intelligent Mining Equipment, Jiangsu Xuzhou 221116, China)

Abstract: As the key component of mine hoisting system, hoisting wire rope is responsible for lifting coal, gangue, personnel and equipment. In the working process, the fretting wear between steel wires will aggravate the fatigue damage of hoisting wire rope, reduce the service life of wire rope, and seriously threaten the safety of the mine hoisting. In order to study the influence of strand structure on the fretting friction and wear characteristics of spiral contact steel wires, the fretting wear tests of steel wires under tension-torsion coupling force were carried out on a self-made test rig. The micro wear characteristics of steel wire surface were observed by the scanning electron microscope (SEM), and the fretting wear mechanism and fracture failure behavior of spiral contact steel wires under different strand structures were revealed. The results show that with the increase of contact force, the frictional coefficient between steel wires under the same diameter contact pairs decreases from 0.748 to 0.646, while that under different diameter contact pairs decreases

Received 20 September 2022, revised 2 January 2023, accepted 3 January 2023, available online 4 January 2023.

*Corresponding author. E-mail: xuchunming@squ.edu.cn, Tel: +86-15162146862.

This project was supported by the Doctoral Starting up Foundation of Suqian University, China (2022XRC039) and the National Natural Science Foundation of China (51975572).

宿迁学院博士科研启动基金(2022XRC039)和国家自然科学基金(51975572)资助.

from 0.941 to 0.911. The friction degree between steel wires under different diameter contact pairs is obviously greater than that under the same diameter contact pairs. In addition, in the stable stage, the friction coefficient between steel wires under the same diameter contact pairs presents a horizontal change trend, while that under different diameter contact pairs shows a slight upward trend. Under different working conditions, the depth and width of wear scars increase with increasing the contact force. For the same contact force, the wear depth of steel wires under the convex contact pairs is significantly greater than that under the concave contact pairs, and the greater the contact force is, the more obvious the difference of wear depth of steel wires under different contact forms is. Whether the diameter of the loading wire and the fatigue wire is the same or not, the wear coefficient of steel wires under different contact forms decreases with the increase of the contact force. The wear depth and coefficient of steel wires under different diameter contact pairs are significantly greater than that under the same diameter contact pairs. For the microscopic wear characteristics of steel wires, compared with the same diameter contact pairs, the worn surface of steel wires under the different diameters contact pairs presents more serious wear characteristics, and the worn surface of steel wires under the concave contact pairs is rougher than that under the convex contact pairs. Furthermore, there are a lot of wear characteristics on the surface of worn steel wire, such as wear debris, material adhesion, plastic deformation, fine scratches, material delamination, micro cracks and furrows. Therefore, the main wear mechanisms between steel wires are abrasive wear, adhesive wear and fatigue wear, and the fatigue wear of steel wires under different diameter contact pairs are more serious, which is caused by the "cutting" effect between thin steel wire and thick steel wire. As the contact force increases, the fatigue life of steel wires under different strand structures decreases gradually. And for the same contact force, the fatigue life of steel wires under different diameter contact pairs is obviously smaller than that under the same diameter contact pairs. The fracture surface of steel wires is obviously divided into fatigue source region, crack propagation region and final fracture region. Abundant secondary cracks and dimples exist in the final fracture region, and the fatigue fracture failure mechanism of steel wires is mainly ductile fracture.

Key words: steel wire; strand structure; fretting wear; wear mechanism; fracture failure

作为矿井提升系统关键部件,提升钢丝绳担负着提升煤炭、矸石、升降人员和设备的任务,一旦提升钢丝绳发生断裂将导致井毁人亡的重大事故。如图1所示,钢丝绳是由钢丝捻绕成股,再以股捻绕成绳的空间螺旋结构体。钢丝绳内部钢丝间接触形式分为凸接触对和凹接触对。由于其内部复杂的接触形式,在矿井提升过程中,提升钢丝绳内部钢丝同时产生拉伸和扭转运动,导致拉伸-扭转耦合力的产生,造成内部钢丝微动磨损。此外,在拉伸、扭转和接触载荷的作用下,钢丝微动磨损区域产生裂纹,形成微动疲劳,促进内部钢丝的疲劳断裂,加剧提升钢丝绳疲劳失效^[1],严重威胁矿井正常生产和人员生命安全。

近年来,一些学者对提升钢丝绳及内部钢丝间摩擦学特性进行了相关研究。彭玉兴等^[2-3]利用自制摩擦试验台分别探究了低温和水油润滑环境下钢丝绳滑动摩擦磨损特性,揭示了层间过渡阶段钢丝绳绕入冲击对绳间摩擦学特性的影响。Chang等^[4-6]总结出钢丝绳间磨损机理主要为黏着磨损、磨粒磨损和疲劳磨损,并利用拉伸破断试验探究了损伤钢丝绳的破断机理。Singh等^[7]发现钢丝绳损坏的主要原因是过度磨损和腐蚀。提升钢丝绳长期服役于恶劣环境中导致内部钢丝发生微动磨损和疲劳断裂,Zhang等^[8-9]利用摩擦

试验台研究了干摩擦下钢丝间微动磨损行为和酸碱腐蚀环境下钢丝电化学腐蚀特性^[10]。Urchegui等^[11-12]采用试验方法分析了不同接触载荷和微动振幅下垂直交叉钢丝微动磨损行为,并提出了基于共焦成像轮廓的微动磨损评估方法,用以分析钢丝磨痕表面特征。为了探究低周疲劳下钢丝间微动疲劳特性,Wang等^[13-16]通过大量钢丝微动疲劳试验,揭示了交叉接触钢丝间摩擦特性、磨损特征以及裂纹扩展规律随微动参数演变规律。Xu等^[17]发现相比于接触载荷,微动振幅对钢丝的磨损特性影响更大,并且探究了矿物颗粒对钢丝间摩擦磨损特性的影响^[18-19]。Cruzado等^[20-21]探讨了接触力和交叉角对钢丝间微动磨损行为的影响,开发了基于ABAQUS的优化算法以准确预测钢丝表面磨痕的演变规律^[22-23]。Meng等^[24]考察了钢丝表面形貌对绳股内部接触性能的影响。Chen等^[25-27]基于弹性接触理论和半解析法对钢丝绳在不同受力状态下内部钢丝间接触性能开展研究,分析了钢丝间接触状态对绳股力学性能的作用机制。Llavori等^[28]提出了预测钢丝疲劳寿命的耦合三维磨损和疲劳数值程序,并通过钢丝微动疲劳试验验证了该程序的可行性。

如图2所示,对于相同型号的钢丝绳,由于其内部绳股由不同排列结构的钢丝捻制而成,存在不同的组

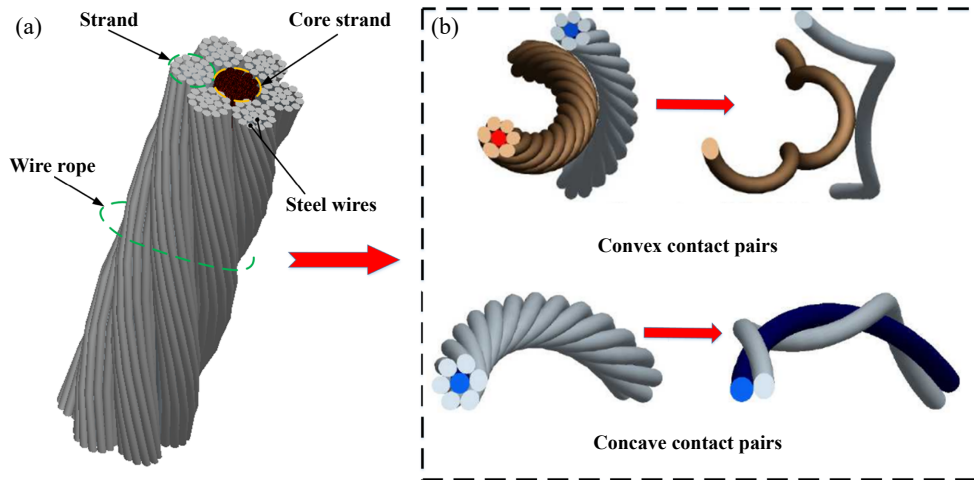


Fig. 1 (a) Structure of wire rope; (b) contact form between steel wires

图 1 (a)钢丝绳结构; (b)钢丝间接触形式

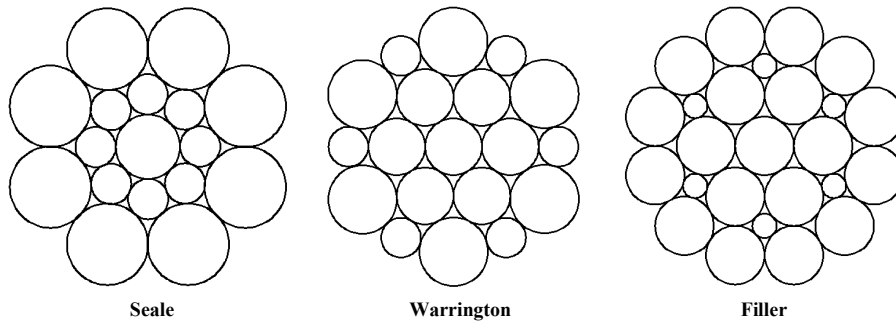


Fig. 2 Common strand structure inside hoisting wire rope

图 2 提升钢丝绳内部常见绳股结构

织结构(填充式、西鲁式、瓦林吞式等), 不同绳股结构内部存在相同钢丝直径接触和不同钢丝直径接触。然而, 之前的研究主要集中于钢丝绳间以及纵向拉伸载荷下相同直径钢丝间摩擦磨损特性, 忽略了钢丝绳内部螺旋接触结构以及钢丝直径对钢丝间微动摩擦磨损特性的影响。因此, 为了探究绳股内部结构形式对钢丝间微动摩擦磨损行为的影响, 开展了拉伸-扭转耦合力作用下螺旋接触钢丝间微动磨损试验, 着重对比研究不同绳股结构下螺旋接触钢丝间摩擦特性、磨损特征以及疲劳断裂失效机理的差异。这些研究和成果对评估钢丝绳使用寿命和保障矿井提升安全提供了重要的基础数据和理论支撑。

1 试验细节

1.1 材料

试验样品为由优质碳素结构钢经冷拔工艺制造而成的细钢丝, 其常被用于制造矿井提升钢丝绳。钢丝的直径分别为1.2和1.4 mm, 杨氏模量为203 GPa,

抗拉强度为1 850 MPa, 屈服强度为1 360 MPa; 钢丝的化学组分(质量分数, w)列于表1中。

1.2 试验原理及参数

为了探究钢丝绳内部螺旋接触钢丝间微动摩擦磨损行为, 在自制的摩擦试验台上开展了钢丝微动磨损试验, 试验台的工作原理如图3所示。钢丝绳内部钢丝间螺旋接触行为被简化为3根钢丝以不同的接触形式相接触, 其中上方的加载钢丝与疲劳钢丝呈凸接触对, 下方的加载钢丝与疲劳钢丝呈凹接触对, 每根钢丝均可以实现往复拉伸和旋转, 通过改变钢丝间接触参数, 可以实现不同工况下钢丝间摩擦磨损行为模拟。

图4所示为自制的摩擦试验台, 其工作流程如下: 凸加载钢丝(18)一端通过步进电机(5)实现往复旋转运动, 另一端通过伺服电动缸(3)实现拉伸运动, 并且凸加载钢丝(18)的张力被拉力传感器(4)实时测得; 凹加载钢丝(19)一端通过步进电机(6)实现往复旋转运动, 另一端穿过凹加载块(7), 通过伺服电动缸(10)实现拉伸运动, 并且凹加载钢丝(19)的张力被拉力传感器

表1 钢丝的化学组分
Table 1 Chemical composition of steel wire

w (Fe)/%	w (Mn)/%	w (Si)/%	w (Ni)/%	w (C)/%	w (S)/%	w (P)/%
98.71	0.42	0.02	0.01	0.83	0.001	<0.001

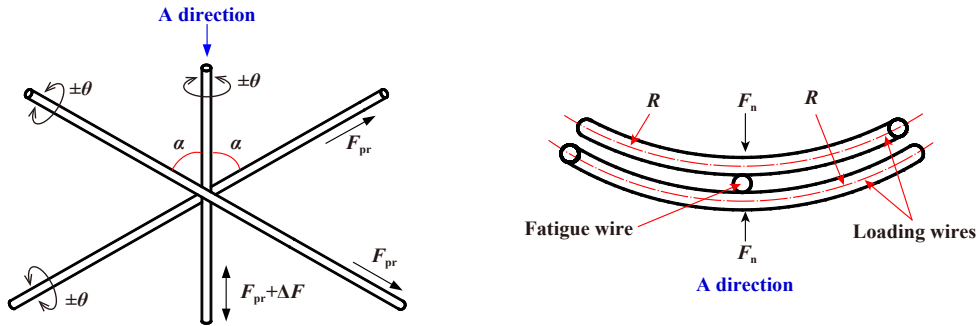
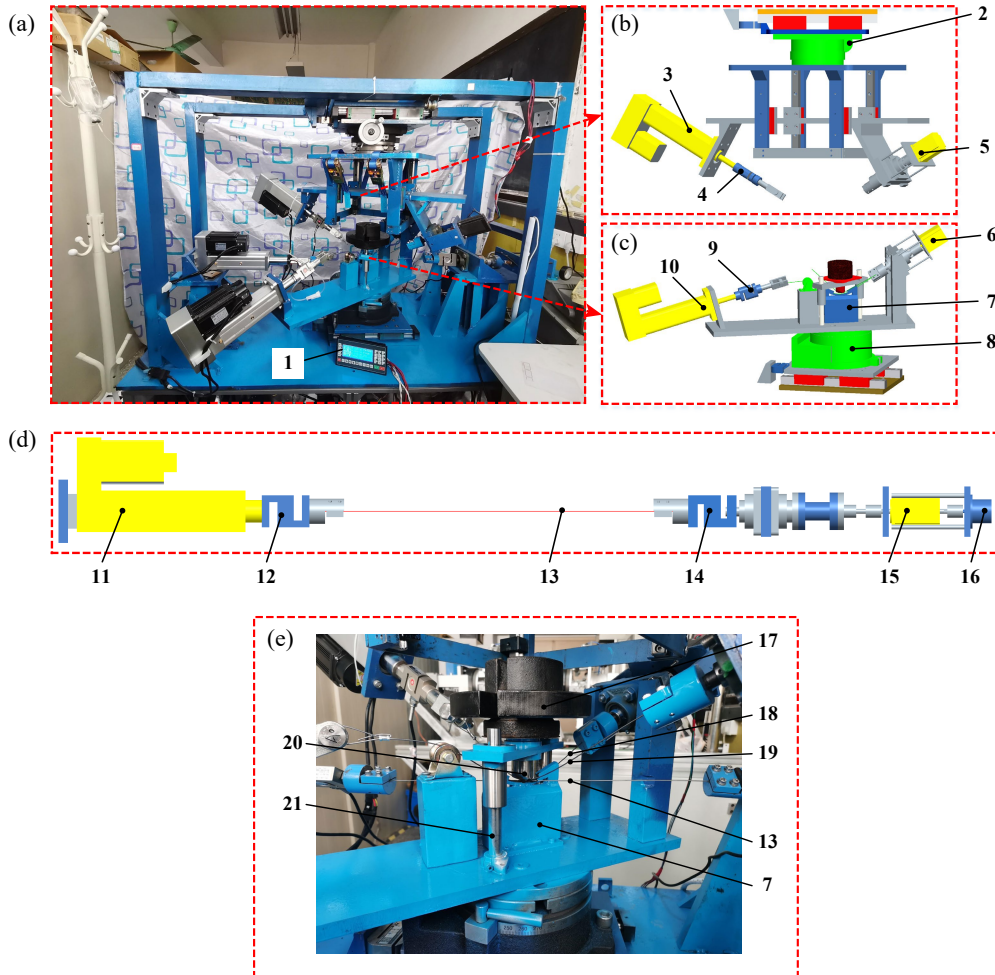


Fig. 3 Working principle of the test rig
图3 试验台的工作原理



1. PLC controller; 2. indexing plate; 3. servo electric cylinder; 4. tension sensor; 5. stepper motor; 6. stepper motor; 7. concave loading block; 8. indexing plate; 9. tension sensor; 10. servo electric cylinder; 11. servo electric cylinder; 12. tension sensor; 13. fatigue wire; 14. tension sensor; 15. stepper motor; 16. angle sensor; 17. counterweight block; 18. convex loading wire; 19. concave loading wire; 20. convex loading block; 21. smooth cylinder

Fig. 4 Self-made friction test rig: (a) overall structure; (b) convex loading mechanism; (c) concave loading mechanism; (d) tension-rotation mechanism; (e) enlarged view of the contact area

图4 自制摩擦试验台: (a)整体结构; (b)凸加载机构; (c)凹加载机构; (d)拉伸-旋转机构; (e)钢丝接触区域放大图

(9)实时测得;疲劳钢丝(13)的一端利用步进电机(15)实现往复旋转,旋转角度通过角度传感器(16)实时测得,另一端在伺服电动缸(11)作用下实现往复拉伸运动,试验过程中疲劳钢丝(13)的两端张力分别通过拉力传感器(12)和(14)实时测得.此外,分别调节分度盘(2)和(8),实现加载钢丝与疲劳钢丝设定的交叉角度.利用PLC控制器(1)控制伺服电动缸对加载钢丝和疲劳钢丝施加初始载荷.之后,对凸加载块(20)顶端平面施加配重块(17),在配重块重力作用下沿着光轴(21)垂直运动,实现加载钢丝与疲劳钢丝紧密接触,钢丝间接触力通过凹加载块(7)底部压力传感器测得.最

后,利用PLC控制器(1)对加载钢丝和疲劳钢丝施加脉冲信号,实现钢丝绳内部不同接触形式钢丝间摩擦磨损行为模拟.

在矿井提升过程中,由于钢丝绳产生振动,导致钢丝绳内部钢丝间接触力产生较大范围的变化^[29].因此,本文作者分别探究了相同直径接触对和不同直径接触对下钢丝间微动摩擦磨损特性随接触力演变规律.其中,相同直径接触对代表疲劳钢丝和加载钢丝的直径均为1.4 mm;不同直径接触对代表疲劳钢丝的直径为1.4 mm,加载钢丝的直径为1.2 mm.详细试验参数列于表2中,每组试验重复3次以确保试验的可重复性.

表 2 试验参数

Table 2 Test parameters

Parameters	Specifications	Parameters	Specifications
Diameter of fatigue wire	1.4 mm	Number of cycles, N	3.0×10^4
Contact force, F_n	40 N; 60 N; 80 N; 100 N	Frequency, f	3.0 Hz
Displacement amplitude, δ	80 μm	Torsion angle, θ	6.0°
Crossing angle, α	30°	Initial tensile force, F_{pr}	500 N
Contact radius, R	50 mm	Temperature	$30 \pm 3^\circ\text{C}$

1.3 分析方法

图5所示为钢丝间摩擦力随时间变化曲线,其通过疲劳钢丝两端的张力差获得.摩擦系数由公式(1)和(2)确定.采用SM-1000三维形貌仪[思显光电技术(上海)有限公司]扫描钢丝磨痕的三维形貌,横向和纵向测量精度均为 $0.1 \mu\text{m}$,垂直方向的最大测量范围为 $1300 \mu\text{m}$,通过其后处理软件Mountains Map获得钢丝的磨损深度和磨损体积.此外,利用扫描电镜(SEM)观察钢丝表面的微观磨损特征.

$$F_{av} = \frac{F_{max} - F_{min}}{2} \quad (1)$$

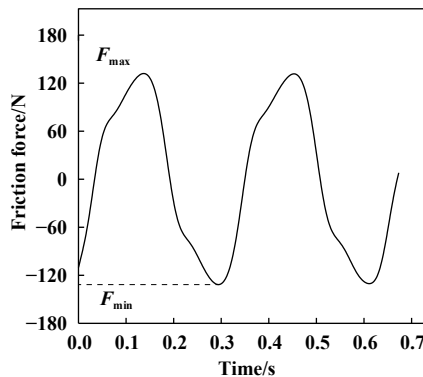


Fig. 5 Variation curve of the frictional force between steel wires with time

图 5 钢丝间摩擦力随时间变化曲线

$$f_{av} = \frac{F_{av}}{2 \times F_n} \quad (2)$$

式中, F_{av} 为摩擦力平均值; f_{av} 为钢丝间摩擦系数; F_n 为钢丝间接触力.

2 结果与讨论

2.1 摩擦系数

图6所示为相同直径接触对下钢丝间摩擦系数随循环次数变化曲线,此时加载钢丝直径为1.4 mm.不同接触力下钢丝间摩擦系数变化曲线均呈现出相同的变化规律:随着循环次数增加,摩擦系数先急剧增加到峰值,然后轻微降低,最后保持相对稳定.因此,钢丝间摩擦系数变化曲线分为3个阶段:快速增长阶段、过渡阶段和稳定阶段.这是因为在摩擦初始阶段,由于钢丝表面膜的保护,钢丝间摩擦力较小.随着循环次数增加,钢丝表面破裂,磨损面积增加,钢丝内部材料直接接触,磨损表面出现黏着和塑性变形,钢丝间摩擦力增加,故摩擦系数迅速增长.随着循环次数进一步增加,摩擦副表面出现大量磨屑,这些磨屑在接触区域起到一定润滑效果,导致钢丝间摩擦力轻微降低,过渡阶段相比于整个试验过程所占的比例较低.在稳定阶段,由于钢丝间接触面积增长速度减缓以及磨屑连续产生和溢出保持动态平衡,最终,钢丝间摩擦系数保持相对稳定变化.图6(b)所示为稳定阶段(后

10000次循环)钢丝间摩擦系数平均值. 随着接触力增加, 钢丝间摩擦系数平均值从0.748减小到0.646, 并且接触力越大, 摩擦系数减小越明显, 这说明钢丝间摩擦力的增长速度小于接触力的增加速度.

图7所示为不同直径接触对下钢丝间摩擦系数随循环次数变化曲线, 此时加载钢丝直径为1.2 mm. 相比于相同直径接触对, 不同直径接触对下钢丝间摩擦系数变化曲线在过渡阶段并不明显, 并且摩擦系数更大. 在稳定阶段, 相同直径接触对下钢丝间摩擦系数呈现出水平变化趋势, 而不同直径接触对下钢丝间摩擦系数呈现出轻微上升趋势. 这是因为疲劳钢丝与加载钢丝的直径不相同, 细钢丝与粗钢丝之间摩擦类似于“切割”现象, 在拉伸-扭转耦合力作用下钢丝接触表面产生挤压和剪切力, 相比于相同直径钢丝间接触, 不同直径钢丝间接触面积更小, 接触应力更大, 钢丝间摩擦更剧烈, 因此摩擦系数更大. 由图7(b)可知, 随着接触力从40 N增加到100 N, 稳定阶段钢丝间摩擦系数平均值从0.941减小到0.911. 不同直径钢丝间

摩擦系数几乎为相同直径钢丝间摩擦系数的1.4倍, 这意味着提升钢丝绳内部不同直径钢丝间接触将会加剧钢丝间摩擦行为.

2.2 磨损深度

图8所示为不同接触形式下钢丝磨痕轮廓随接触力演变规律. 不同工况下钢丝磨痕轮廓呈现弧形凹坑, 磨痕轮廓表面较为粗糙. 此外, 随着接触力增加, 钢丝磨痕深度随之增加, 并且磨痕宽度呈现出轻微增长趋势. 这是因为钢丝间相互摩擦, 引起接触区域表面材料脱落, 磨痕表面出现各种微观磨损特征, 导致磨痕轮廓粗糙不光滑. 随着接触力增加, 钢丝间接触应力增大, 钢丝表面磨损剧烈, 造成钢丝磨痕深度和宽度增加.

通过对图8所示不同工况下钢丝磨痕轮廓的最大磨损深度统计, 获得不同接触形式下钢丝最大磨损深度随接触力演变规律, 如图9所示. 对于相同直径接触对, 随着接触力增加, 凸接触对下钢丝磨损深度从156.02 μm 增加到236.18 μm ; 凹接触对下钢丝磨损深

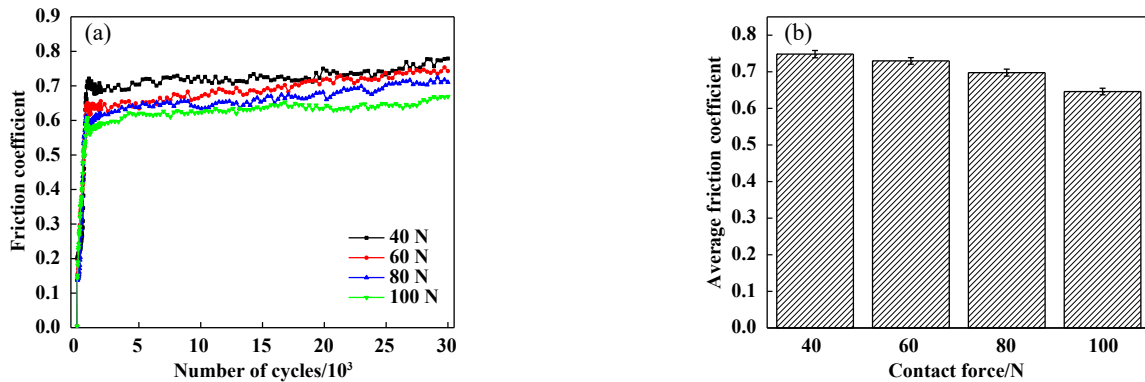


Fig. 6 Variation of the frictional coefficient between steel wires with contact force under the same diameter contact pairs: (a) change curve of the frictional coefficient; (b) average value of the frictional coefficient

图6 相同直径接触对下钢丝间摩擦系数随接触力变化规律: (a)摩擦系数变化曲线; (b)摩擦系数平均值

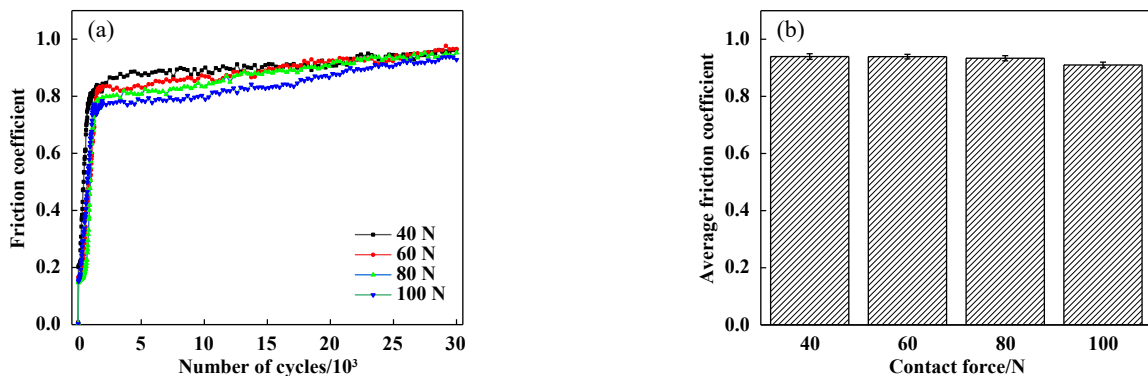


Fig. 7 Variation of the frictional coefficient between steel wires with contact force under different diameter contact pairs: (a) change curve of the frictional coefficient; (b) average value of the frictional coefficient

图7 不同直径接触对下钢丝间摩擦系数随接触力变化规律: (a)摩擦系数变化曲线; (b)摩擦系数平均值

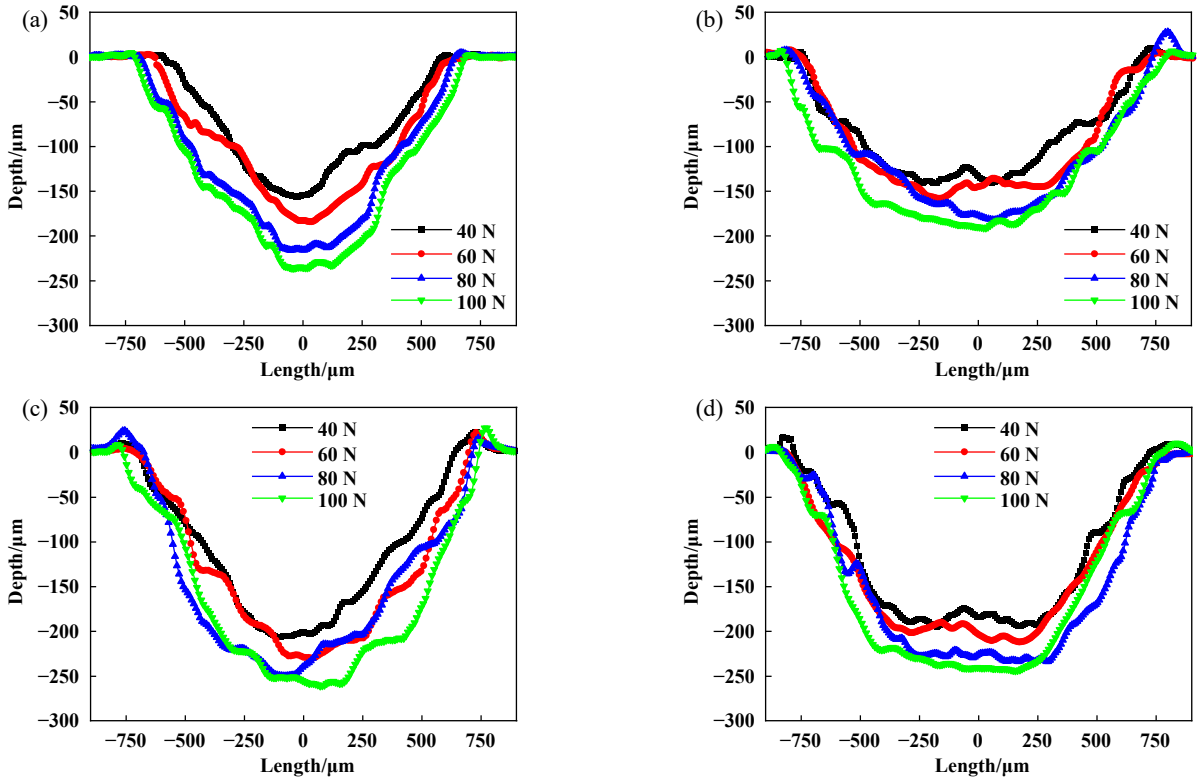


Fig. 8 Change law of wear scar profile of steel wire with contact force under different contact forms: (a) same diameter contact pairs - convex contact pairs; (b) same diameter contact pairs - concave contact pairs; (c) different diameter contact pairs - convex contact pairs; (d) different diameter contact pairs - concave contact pairs

图 8 不同接触形式下钢丝磨损轮廓随接触力变化规律: (a)相同直径接触对-凸接触对; (b)相同直径接触对-凹接触对; (c)不同直径接触对-凸接触对; (d)不同直径接触对-凹接触对

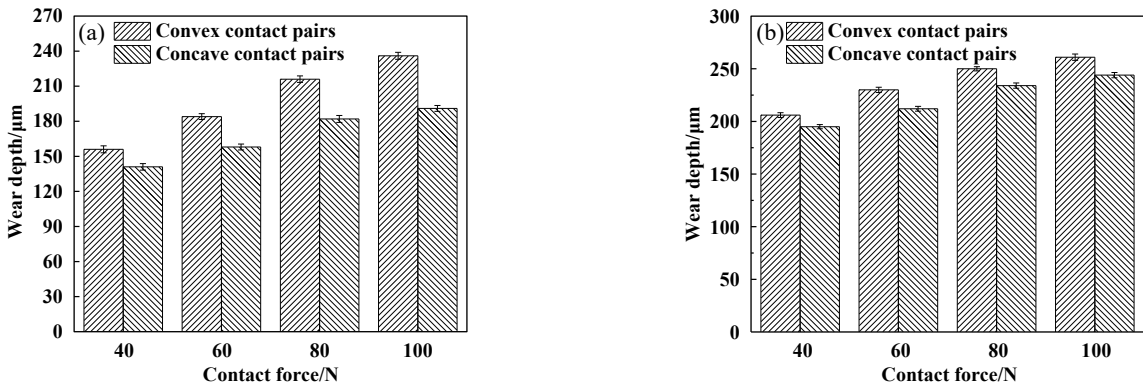


Fig. 9 Variation of the wear depth of steel wire with contact force under different contact forms: (a) same diameter contact pairs; (b) different diameter contact pairs

图 9 不同接触形式下钢丝磨损深度随接触力变化规律: (a)相同直径接触对; (b)不同直径接触对

度从141.49 μm 增加到191.26 μm . 对于不同直径接触对, 随着接触力增加, 凸接触对下钢丝磨损深度从206.53 μm 增加到261.42 μm ; 凹接触对下钢丝磨损深度从195.34 μm 增加到244.02 μm . 此外, 对于相同接触力, 凸接触对下钢丝磨损深度明显大于凹接触对下钢丝磨损深度, 并且接触力越大, 不同接触形式下钢丝磨损深度差距越明显. 这是因为随着接触力增加, 钢

丝间接触应力越大, 钢丝磨损越严重. 并且, 凸接触对下钢丝间接触应力大于凹接触对下钢丝间接触应力^[18], 因此凸接触对下钢丝表面产生更加严重的磨损. 另外, 相比于相同直径接触对, 不同直径接触对下钢丝的磨损深度更深, 这是因为不同直径钢丝间摩擦类似于“切割”现象, 接触区域的接触应力更大, 加剧了钢丝的磨损.

2.3 磨损系数

材料的耐磨性能可以通过磨损系数反映, 钢丝表面的磨损系数由公式(3)计算获得^[30].

$$k = \frac{W_v}{2 \cdot \delta \cdot N \cdot F_n} \quad (3)$$

式中, W_v 为磨损体积, 单位为 mm^3 .

图10所示为不同接触形式下钢丝磨损系数随接触力演变规律. 由图10可知, 不管加载钢丝与疲劳钢丝的直径是否相同, 不同接触形式下钢丝的磨损系数均随着接触力增加而减小. 由于钢丝的磨损系数与磨损体积成正比, 与接触力成反比, 所以钢丝的磨损系数随着接触力增加而减小意味着钢丝磨损体积的增长速度小于接触力的增加速度. 即接触力越大, 单位距离下单位载荷造成的磨损量却越小. 此外, 凸接触对下钢丝的磨损深度和磨损系数明显大于凹接触对下钢丝的磨损深度和磨损系数, 并且不同直径接触对下钢丝的磨损程度明显大于相同直径接触对下钢丝的磨损程度. 此外, 随着接触力增加, 相同直径接触对

下钢丝间磨损系数缓慢减小, 而不同直径接触对下钢丝间磨损系数呈现出线性降低趋势. 这是因为相比于相同直径钢丝间摩擦, 不同直径钢丝间接触应力更大, 磨损越剧烈. 当钢丝间磨损面积增加到一定程度, 磨损速率降低, 接触力增加对磨损体积增长的影响减弱, 因此不同直径接触对下钢丝间磨损系数降低趋势更加明显, 这也意味着提升钢丝绳内部不同直径钢丝间接触, 将会更容易产生严重的材料损伤, 导致钢丝绳的使用寿命降低.

2.4 磨损机理

图11和图12分别所示为凸接触对和凹接触对下钢丝表面磨痕宏观形貌的SEM照片. 可以看出, 不同工况下钢丝磨痕均呈现椭圆形的凹坑, 磨痕边缘出现塑性变形和材料堆积现象, 并伴有高低不平的磨痕形貌. 此外, 相比于相同直径接触对, 不同直径接触对下钢丝磨痕表面呈现出更严重的磨损特征, 并且凹接触对下磨痕表面比凸接触对下磨痕表面更加粗糙.

图13所示为凸接触对下钢丝磨痕表面的微观磨

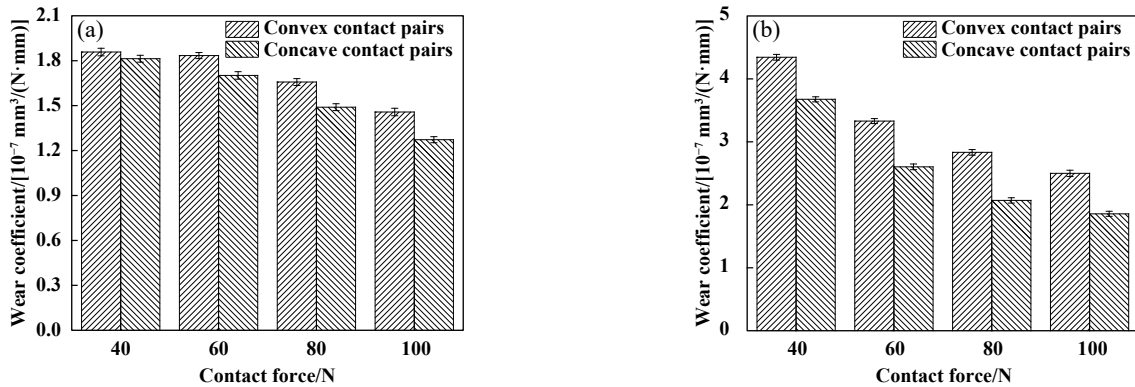


Fig. 10 Variation of the wear coefficient of steel wire with contact force under different contact forms: (a) same diameter contact pairs; (b) different diameter contact pairs

图10 不同接触形式下钢丝磨损系数随接触力变化规律: (a)相同直径接触对; (b)不同直径接触对

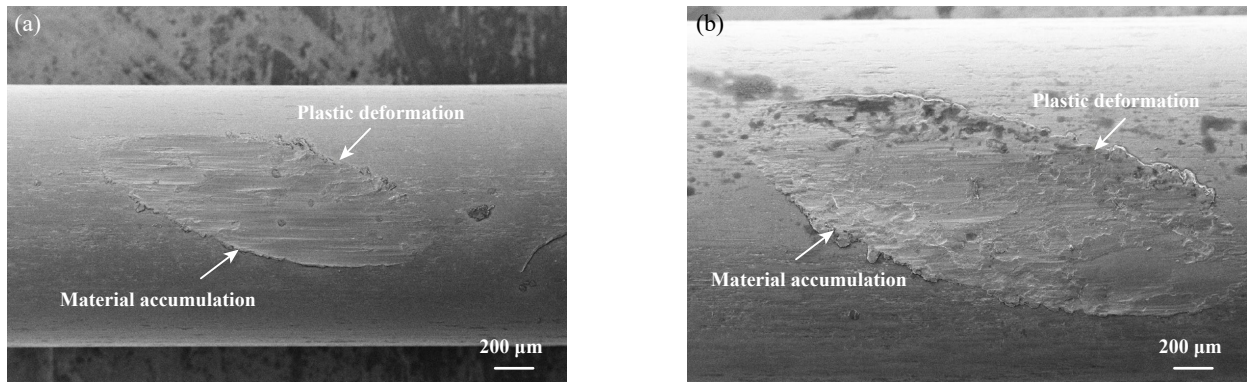


Fig. 11 SEM micrographs of morphology of wear scars under the convex contact pairs: (a) same diameter contact pairs; (b) different diameter contact pairs

图11 凸接触对下钢丝磨痕宏观形貌的SEM照片: (a)相同直径接触对; (b)不同直径接触对

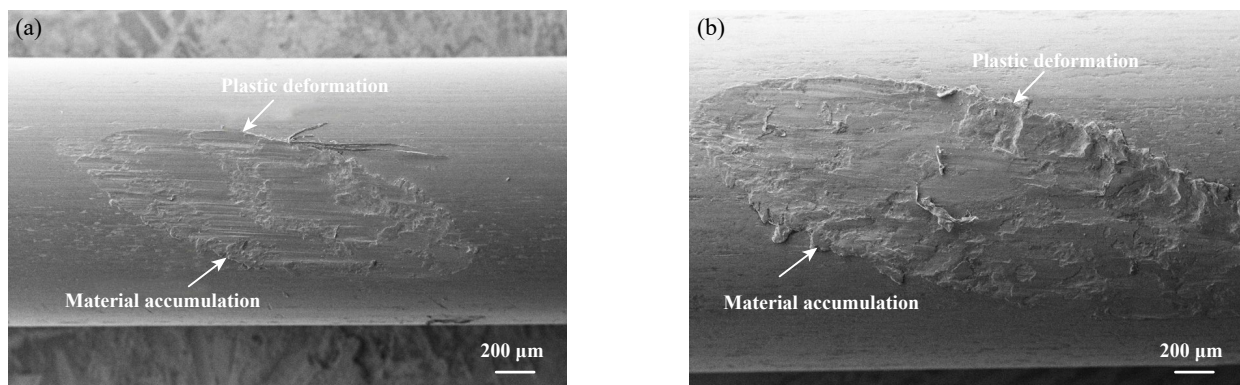


Fig. 12 SEM micrographs of macro morphology of wear scars under the concave contact pairs:
(a) same diameter contact pairs; (b) different diameter contact pairs

图 12 凹接触对下钢丝磨痕宏观形貌的SEM照片:(a)相同直径接触对;(b)不同直径接触对

损特征. 由图13可知, 不同工况下钢丝磨痕表面出现大量的磨屑、材料黏附、塑性变形、细划痕、材料分层、微小裂纹以及沿滑动方向的犁沟等微观磨损特征. 这是因为钢丝间相互摩擦产生磨屑, 在挤压和相对滑动作用下磨屑对接触表面进行切削, 导致犁沟现象. 此外, 在挤压、剪切以及扭转复合载荷作用下, 磨痕表面的微凸峰不断接触而发生弹塑性变形和黏着, 黏附于接触表面的磨屑在挤压和切向力的作用下划伤钢丝表面, 造成细划痕. 随着循环次数增加, 钢丝表面材料受到循环反复的法向和切向力, 导致磨痕的次表层产生剪切应力, 促进了微裂纹的萌生和横向扩展, 当次表层的裂纹相互连接后, 材料以剥层的形式脱落, 从而形成片状磨屑、微小裂纹以及阶梯状材料分层. 此外, 相比于相同直径接触对, 不同直径接触对下钢丝表面分布着更加严重的微小裂纹和材料分层现象. 这是因为在摩擦过程中, 由于细钢丝对粗钢丝的切削效果和拉伸、挤压、剪切以及扭转复合力作用, 钢丝表面产生复杂的接触应力状态, 导致磨痕表面出现严重的疲劳磨损特征. 此外, 随着接触力增加, 钢丝间接触应力增大, 钢丝表面疲劳磨损越严重, 钢丝的磨损深度和磨损体积增加, 并且带有部分磨粒磨损特征的表层材料以剥层的形式从磨痕表面脱落, 所以磨粒磨损特征随着接触力增加轻微降低. 因此, 凸接触对下钢丝间主要磨损机理为磨粒磨损、黏着磨损和疲劳磨损, 并且不同直径接触对下钢丝表面疲劳磨损特征更加严重.

图14所示为凹接触对下钢丝磨痕表面的微观磨损特征. 由图14可以看出, 不同工况下钢丝磨痕表面同样呈现出大量的磨屑、塑性变形、材料分层、凹坑、材料黏附、微小裂纹以及犁沟等微观磨损特征. 相比

于凸接触对, 凹接触对下钢丝磨损区域存在更加明显的微小裂纹和材料分层现象. 这是因为凹接触对下钢丝间磨屑不易于被排出, 在挤压、剪切以及扭转力的作用下对磨痕表面产生应力集中现象, 加剧钢丝表面的疲劳磨损, 导致微小裂纹和材料分层现象更加显著. 并且凹接触下钢丝间接触应力小于凸接触对下钢丝间接触应力, 钢丝间摩擦不充分, 同样会造成钢丝表面磨损特征更多, 而磨损深度和磨损体积更小. 此外, 不同直径钢丝间接摩擦呈现出更加严重的疲劳磨损特征, 这是由于细钢丝与粗钢丝间“切削”效果导致的. 综上所述, 凹接触对下钢丝间主要磨损机理为磨粒磨损、疲劳磨损和黏着磨损, 并且不同直径接触对下钢丝表面同样呈现出更加严重的疲劳磨损特征.

2.5 疲劳断裂机理

提升钢丝绳内部钢丝长期承受循环往复的拉伸和扭转载荷, 从而不可避免地发生疲劳断裂现象. 之前的研究主要集中于钢丝间微动摩擦磨损特性, 无法观察到钢丝内部裂纹扩展情况和最终疲劳断裂失效机理. 因此, 探究钢丝疲劳断裂失效机理对评估钢丝绳的承载能力和服役寿命具有重要意义.

图15所示为不同绳股结构下钢丝疲劳寿命随接触力演变规律. 可以发现, 钢丝疲劳寿命随着接触力增加而减小. 这是因为随着接触力增加, 钢丝表面磨损越严重, 并且疲劳钢丝受到循环往复的拉伸和扭转载荷, 在磨损区域产生裂纹, 越大的接触应力促进了钢丝内部裂纹扩展, 导致钢丝疲劳寿命降低. 此外, 对于相同的接触力, 不同直径接触对下钢丝疲劳寿命明显小于相同直径接触对下钢丝疲劳寿命. 这是因为不同直径钢丝间摩擦类似于“切割”现象, 钢丝接触表面材料损失明显. 在拉伸-扭转复合力作用下钢丝接触表

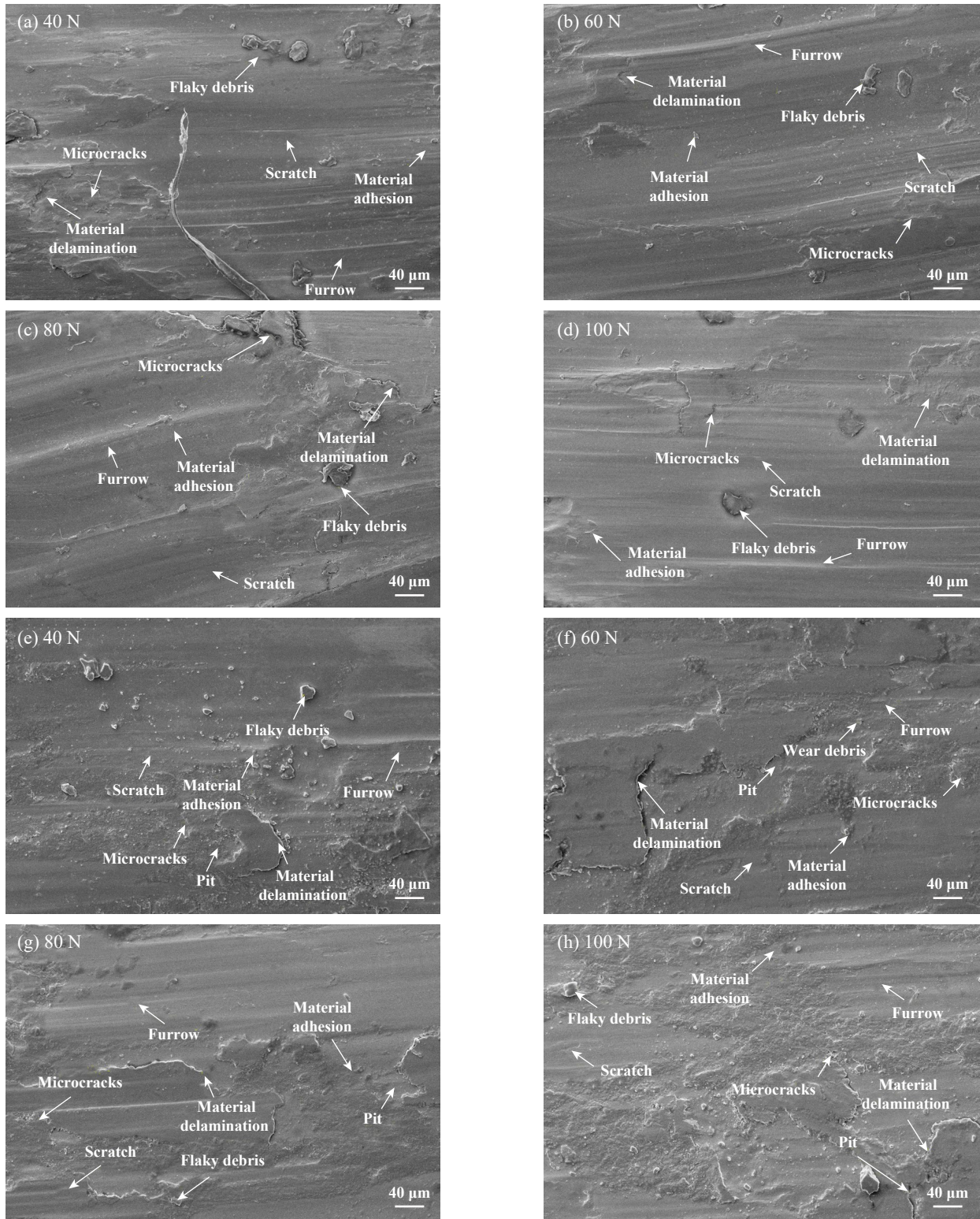


Fig. 13 SEM micrographs of micro morphology of wear scars under the convex contact pairs: (a~d) same diameter contact pairs; (e~h) different diameter contact pairs

图13 凸接触对下钢丝磨痕的微观形貌的SEM照片:(a~d)相同直径接触对;(e~h)不同直径接触对

面产生更大的接触应力和剪切应力,促进了内部裂纹的萌生与扩展,因此钢丝疲劳寿命更小,这可由图16中钢丝断口的裂纹扩展区所占的比例更大证实。

图16所示为接触力100 N时钢丝疲劳断口宏观形貌的SEM照片。由图16可以发现,钢丝断口没有明显的颈缩和变形,断口边缘存在不明显的剪切唇。其中,

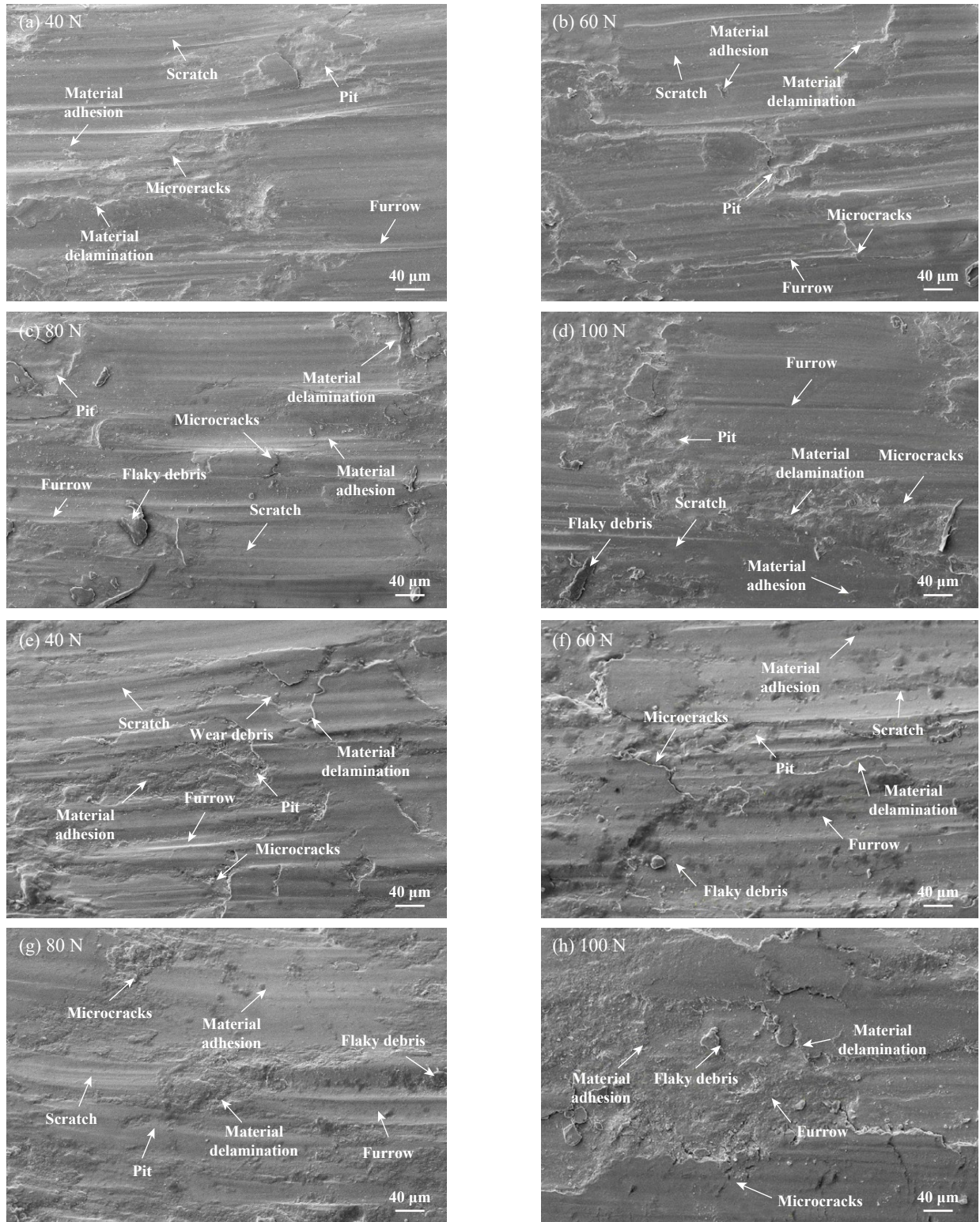


Fig. 14 SEM micrographs of micro morphology of wear scars under the concave contact pairs: (a~d) same diameter contact pairs; (e~h) different diameter contact pairs

图 14 凹接触对下钢丝磨痕微观形貌的SEM照片:(a~d)相同直径接触对;(e~h)不同直径接触对

区域A为疲劳源区,在摩擦过程中,该区域出现磨损缺口,在持续的挤压、剪切以及交变应力的作用下,钢丝磨痕表面产生应力集中,促进了裂纹的萌生.区域

B为裂纹扩展区,该区域裂纹沿着与正应力垂直方向扩展,在循环交变应力作用下,裂纹扩展区反复张开、闭合和相互摩擦,导致裂纹扩展区表面较为光滑.区

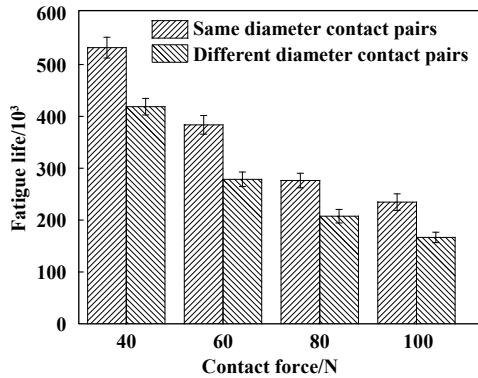


Fig. 15 Variation of the fatigue life of steel wire with contact force under different rope strand structures

图15 不同绳股结构下钢丝疲劳寿命随接触力演变

域C为瞬断区,当裂纹扩展到一定程度时,主断面的有效承载面积不足以支撑循环应力,钢丝在瞬断区断裂,该区域形貌高低不平、表面粗糙。相比于相同直径接触对,不同直径接触对下断口的裂纹扩展区占总面积的比例更大,放射裂纹几乎布满整个断口表面。这是因为不同直径钢丝间摩擦将会引起更大的接

触应力,与剪切应力和循环交变应力一起导致钢丝内部产生复杂的应力状态,从而促进钢丝内部裂纹的扩展。

图17所示为钢丝疲劳断口裂纹扩展区微观形貌的SEM照片。由图17可以发现,裂纹扩展区表面较为光滑平整,分布着大量的小凹坑和碎屑,疲劳辉纹不明显。这是因为在疲劳试验中,钢丝内部裂纹扩展区经历循环往复的张开和闭合,断口表面反复接触和研磨,导致该区域产生大量的细小碎屑,并在挤压和扭转力的作用下切削接触表面,造成断口表面出现大量的小凹坑,并且疲劳辉纹在研磨过程中被覆盖,表现不明显^[31]。

图18所示钢丝疲劳断口瞬断区微观形貌的SEM照片。由图18可以发现,钢丝断口的瞬断区呈现出纤维状,并且断口表面分布着大量的韧窝以及二次裂纹,这是由于疲劳裂纹失稳扩展时在瞬断区所形成的,并随着疲劳裂纹扩展而不断增多^[32]。因此,钢丝疲劳断裂失效机理主要为韧性断裂。

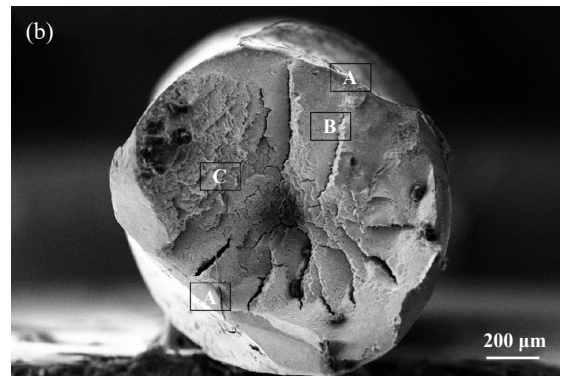
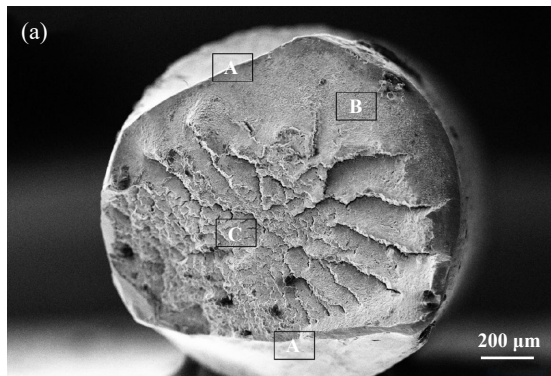


Fig. 16 SEM micrographs of micro morphology of fatigue fracture of steel wire:

(a) same diameter contact pairs; (b) different diameter contact pairs

图16 钢丝疲劳断口宏观形貌的SEM照片:(a)相同直径接触对;(b)不同直径接触对

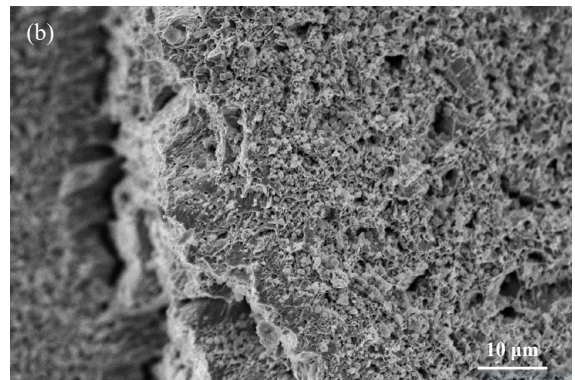


Fig. 17 SEM micrographs of micro morphology of crack propagation region of fatigue fractograph:

(a) same diameter contact pairs; (b) different diameter contact pairs

图17 钢丝疲劳断口裂纹扩展区微观形貌的SEM照片:(a)相同直径接触对;(b)不同直径接触对

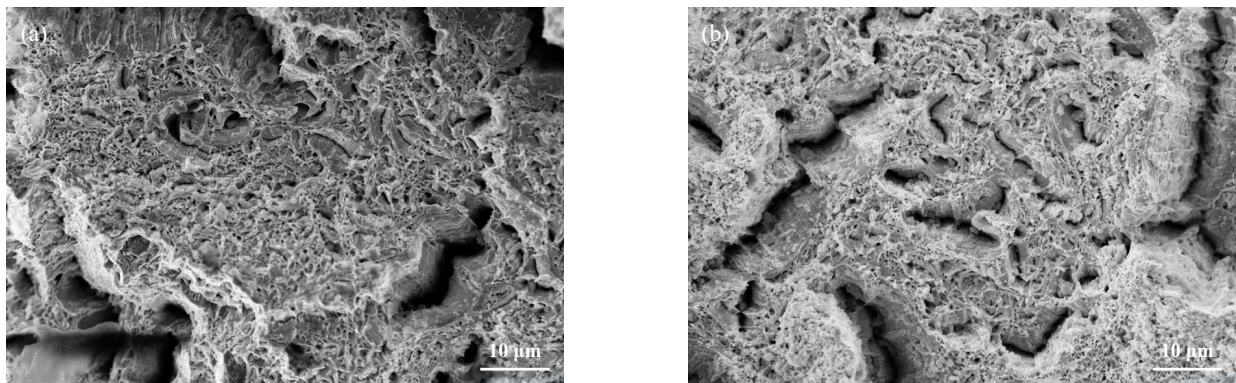


Fig. 18 SEM micrographs of micro morphology of final fracture region of fatigue fractograph: (a) same diameter contact pairs; (b) different diameter contact pairs

图 18 钢丝疲劳断口瞬断区微观形貌的SEM照片:(a)相同直径接触对;(b)不同直径接触对

3 结论

a. 随着接触力增加, 相同直径接触对下钢丝间摩擦系数从0.748减小到0.646, 不同直径接触对下钢丝间摩擦系数0.941减小到0.911, 不同直径钢丝间摩擦系数明显大于相同直径钢丝间摩擦系数; 稳定阶段, 相同直径接触对下钢丝间摩擦系数保持相对水平变化, 而不同直径接触对下钢丝间摩擦系数曲线呈现出轻微上升趋势。

b. 随着接触力增加, 钢丝磨损深度增加, 而磨损系数却逐渐降低; 相比于凹接触对, 凸接触对下钢丝表面磨损程度更大, 并且不同直径接触对下钢丝的磨损程度明显大于相同直径接触对下钢丝的磨损程度, 这意味着提升钢丝绳内部不同直径钢丝间接触, 将会产生更加严重的材料损伤。

c. 不同工况下钢丝间主要磨损机理为磨粒磨损、黏着磨损和疲劳磨损, 并且不同直径接触对下钢丝磨损表面的疲劳磨损特征更加严重; 钢丝疲劳断口表面呈现出疲劳源区、裂纹扩展区和瞬断区, 其中裂纹扩展区表面光滑, 观察不到明显的疲劳辉纹, 而瞬断区存在大量二次裂纹和韧窝形貌, 钢丝疲劳断裂失效机理主要为韧性断裂。

参考文献

- [1] Périer V, Dieng L, Gaillet L, et al. Fretting-fatigue behaviour of bridge engineering cables in a solution of sodium chloride[J]. *Wear*, 2009, 267(1-4): 308–314. doi: [10.1016/j.wear.2008.12.107](https://doi.org/10.1016/j.wear.2008.12.107).
- [2] Peng Yuxing, Wang Gaofang, Zhu Zhencai, et al. Friction and wear characteristics of mine hoist wire rope at low temperature[J]. *Tribology*, 2022, 42(3): 552–561 (in Chinese) [彭玉兴, 王高芳, 朱真才, 等. 低温环境下矿井提升钢丝绳摩擦磨损特性研究[J]. *摩擦学学报*, 42(3), 2022, 42(3): 552–561]. doi: [10.16078/j.tribology.2021088](https://doi.org/10.16078/j.tribology.2021088).
- [3] Peng Yuxing, Sun Shisheng, Zhu Zhencai, et al. Winding-in impact friction characteristics of wire rope in winding hoist[J]. *Tribology*, 2017, 37(1): 90–98 (in Chinese) [彭玉兴, 孙士生, 朱真才, 等. 缠绕提升钢丝绳绕入冲击摩擦特性研究[J]. *摩擦学学报*, 2017, 37(1): 90–98]. doi: [10.16078/j.tribology.2017.01.012](https://doi.org/10.16078/j.tribology.2017.01.012).
- [4] Chang Xiangdong, Peng Yuxing, Zhu Zhencai, et al. Effects of strand lay direction and crossing angle on tribological behavior of winding hoist rope[J]. *Materials*, 2017, 10(6): 630. doi: [10.3390/ma10060630](https://doi.org/10.3390/ma10060630).
- [5] Chang Xiangdong, Peng Yuxing, Zhu Zhencai, et al. Effect of wear scar characteristics on the bearing capacity and fracture failure behavior of winding hoist wire rope[J]. *Tribology International*, 2019, 130: 270–283. doi: [10.1016/j.triboint.2018.09.023](https://doi.org/10.1016/j.triboint.2018.09.023).
- [6] Chang Xiangdong, Huang Haibo, Peng Yuxing, et al. Friction, wear and residual strength properties of steel wire rope with different corrosion types[J]. *Wear*, 2020, 458–459: 203425. doi: [10.1016/j.wear.2020.203425](https://doi.org/10.1016/j.wear.2020.203425).
- [7] Singh R P, Mallick M, Verma M K. Studies on failure behaviour of wire rope used in underground coal mines[J]. *Engineering Failure Analysis*, 2016, 70: 290–304. doi: [10.1016/j.engfailanal.2016.09.002](https://doi.org/10.1016/j.engfailanal.2016.09.002).
- [8] Zhang Dekun, Geng Hao, Zhang Zefeng, et al. Investigation on the fretting fatigue behaviors of steel wires under different strain ratios[J]. *Wear*, 2013, 303(1–2): 334–342. doi: [10.1016/j.wear.2013.03.020](https://doi.org/10.1016/j.wear.2013.03.020).
- [9] Zhang Dekun, Shen Yan, Xu Linmin, et al. Fretting wear behaviors of steel wires in coal mine under different corrosive mediums[J]. *Wear*, 2011, 271(5–6): 866–874. doi: [10.1016/j.wear.2011.03.028](https://doi.org/10.1016/j.wear.2011.03.028).
- [10] Shen Yan, Zhang Dekun, Ge Shirong. Effect of fretting amplitudes on fretting wear behavior of steel wires in coal mines[J]. *Mining Science and Technology (China)*, 2010, 20(6): 803–808. doi: [10.1016/S1674-5264\(09\)60285-4](https://doi.org/10.1016/S1674-5264(09)60285-4).
- [11] Urchegui M A, Hartelt M, Klaffke D, et al. Laboratory fretting tests with thin wire specimens[J]. *Tribotest*, 2007, 13(2): 67–81. doi: [10.1002/tt.34](https://doi.org/10.1002/tt.34).

- [12] Mitchell M R, Link R E, Urchegui M A, et al. A method for evaluating fretting wear scars in thin steel roping wires based on confocal imaging profilometry[J]. *Journal of Testing and Evaluation*, 2007, 35(4): 100631. doi: [10.1520/jte100631](https://doi.org/10.1520/jte100631).
- [13] Wang Dagang, Zhu Zhencai, Song Daozhu. Effects of tensile stress ratio and amplitude on tension-torsion fretting-corrosion-fatigue behaviors of non-perpendicularly crossed steel wires[J]. *Engineering Failure Analysis*, 2020, 117: 104839. doi: [10.1016/j.engfailanal.2020.104839](https://doi.org/10.1016/j.engfailanal.2020.104839).
- [14] Wang Xiangru, Wang Dagang, Li Xiaowu, et al. Comparative analyses of torsional fretting, longitudinal fretting and combined longitudinal and torsional fretting behaviors of steel wires[J]. *Engineering Failure Analysis*, 2018, 85: 116–125. doi: [10.1016/j.engfailanal.2017.12.002](https://doi.org/10.1016/j.engfailanal.2017.12.002).
- [15] Wang Xiangru, Wang Dagang, Zhang Dekun, et al. Effect of torsion angle on tension-torsion multiaxial fretting fatigue behaviors of steel wires[J]. *International Journal of Fatigue*, 2018, 106: 159–164. doi: [10.1016/j.ijfatigue.2017.09.021](https://doi.org/10.1016/j.ijfatigue.2017.09.021).
- [16] Wang Dagang, Zhang Dekun, Ge Shirong. Effect of displacement amplitude on fretting fatigue behavior of hoisting rope wires in low cycle fatigue[J]. *Tribology International*, 2012, 52: 178–189. doi: [10.1016/j.triboint.2012.04.008](https://doi.org/10.1016/j.triboint.2012.04.008).
- [17] Xu Chunming, Peng Yuxing, Zhu Zhencai, et al. Fretting friction and wear of steel wires in tension-torsion and helical contact form[J]. *Wear*, 2019, 432–433: 202946. doi: [10.1016/j.wear.2019.202946](https://doi.org/10.1016/j.wear.2019.202946).
- [18] Xu Chunming, Peng Yuxing, Zhu Zhencai, et al. Fretting behavior evolution of steel wires with helical structure after adding ore particles in lubricating grease[J]. *Engineering Failure Analysis*, 2021, 124: 105332. doi: [10.1016/j.engfailanal.2021.105332](https://doi.org/10.1016/j.engfailanal.2021.105332).
- [19] Xu Chunming, Peng Yuxing, Zhu Zhencai, et al. Influence of different mineral particles in lubricating grease on the fretting behavior between steel wires under different contact forms[J]. *Wear*, 2021, 472–473: 203700. doi: [10.1016/j.wear.2021.203700](https://doi.org/10.1016/j.wear.2021.203700).
- [20] Cruzado A, Hartelt M, Wäsche R, et al. Fretting wear of thin steel wires. Part 1: influence of contact pressure[J]. *Wear*, 2010, 268(11–12): 1409–1416. doi: [10.1016/j.wear.2010.02.017](https://doi.org/10.1016/j.wear.2010.02.017).
- [21] Cruzado A, Hartelt M, Wäsche R, et al. Fretting wear of thin steel wires. Part 2: influence of crossing angle[J]. *Wear*, 2011, 273(1): 60–69. doi: [10.1016/j.wear.2011.04.012](https://doi.org/10.1016/j.wear.2011.04.012).
- [22] Cruzado A, Leen S B, Urchegui M A, et al. Finite element simulation of fretting wear and fatigue in thin steel wires[J]. *International Journal of Fatigue*, 2013, 55: 7–21. doi: [10.1016/j.ijfatigue.2013.04.025](https://doi.org/10.1016/j.ijfatigue.2013.04.025).
- [23] Cruzado A, Urchegui M A, Gómez X. Finite element modeling of fretting wear scars in the thin steel wires: application in crossed cylinder arrangements[J]. *Wear*, 2014, 318(1–2): 98–105. doi: [10.1016/j.wear.2014.06.019](https://doi.org/10.1016/j.wear.2014.06.019).
- [24] Meng Fanming, He Jing, Gong Xiansheng. Influence of wire's surface topography on interwire contact performance of simple spiral strand[J]. *Industrial Lubrication and Tribology*, 2018, 70(6): 961–976. doi: [10.1108/ilt-04-2017-0096](https://doi.org/10.1108/ilt-04-2017-0096).
- [25] Chen Yuanpei, Meng Fanming, Gong Xiansheng. Interwire wear and its influence on contact behavior of wire rope strand subjected to cyclic bending load[J]. *Wear*, 2016, 368–369: 470–484. doi: [10.1016/j.wear.2016.10.020](https://doi.org/10.1016/j.wear.2016.10.020).
- [26] Chen Yuanpei, Meng Fanming, Gong Xiansheng. Full contact analysis of wire rope strand subjected to varying loads based on semi-analytical method[J]. *International Journal of Solids and Structures*, 2017, 117: 51–66. doi: [10.1016/j.ijsolstr.2017.04.004](https://doi.org/10.1016/j.ijsolstr.2017.04.004).
- [27] Meng Fanming, Chen Yuanpei, Du Minggang, et al. Study on effect of inter-wire contact on mechanical performance of wire rope strand based on semi-analytical method[J]. *International Journal of Mechanical Sciences*, 2016, 115–116: 416–427. doi: [10.1016/j.ijmecsci.2016.07.012](https://doi.org/10.1016/j.ijmecsci.2016.07.012).
- [28] Llavori I, Zabala A, Mendiguren J, et al. A coupled 3D wear and fatigue numerical procedure: application to fretting problems in ultra-high strength steel wires[J]. *International Journal of Fatigue*, 2021, 143: 106012. doi: [10.1016/j.ijfatigue.2020.106012](https://doi.org/10.1016/j.ijfatigue.2020.106012).
- [29] Wang Dagang, Zhang Dekun, Zhang Zefeng, et al. Effect of various kinematic parameters of mine hoist on fretting parameters of hoisting rope and a new fretting fatigue test apparatus of steel wires[J]. *Engineering Failure Analysis*, 2012, 22: 92–112. doi: [10.1016/j.engfailanal.2012.01.008](https://doi.org/10.1016/j.engfailanal.2012.01.008).
- [30] Challen J M, Oxley P L B, Hockenhuil B S. Prediction of Archard's wear coefficient for metallic sliding friction assuming a low cycle fatigue wear mechanism[J]. *Wear*, 1986, 111(3): 275–288. doi: [10.1016/0043-1648\(86\)90188-2](https://doi.org/10.1016/0043-1648(86)90188-2).
- [31] Wang Rong. Failure mechanism analysis and countermeasures[M]. Beijing: China Machine Press, 2020: 38–127 (in Chinese) [王荣. 失效机理分析与对策[M]. 北京: 机械工业出版社, 2020: 38–127].
- [32] Chan K S. Roles of microstructure in fatigue crack initiation[J]. *International Journal of Fatigue*, 2010, 32(9): 1428–1447. doi: [10.1016/j.ijfatigue.2009.10.005](https://doi.org/10.1016/j.ijfatigue.2009.10.005).